A Consequence Model for Bentonite Buffer Defects in Fractured Rock

Stuart Stothoff

Center for Nuclear Waste Regulatory Analyses, 6220 Culebra Rd., San Antonio, TX, 78238; sstothoff@swri.org

One design concept for geologic repositories surrounds emplaced high-level radioactive waste canisters with a swelling bentonite buffer in order to (i) isolate the waste package from potentially corrosive formation waters, (ii) limit releases from failed waste packages, and (iii) support the waste packages during seismic and tectonic disturbances. The isolation function of diffusion-dominated transport in self-healing bentonite can be so dominant that performance is insensitive to the role of the barrier with respect to other factors. A consequence model that considers defects or gaps in the bentonite buffer consistent with the natural system, allowing preferential transport of oxidants and released radionuclides through the bentonite, provides a reasonable method for identifying the barrier role of the natural system. Copper corrosion rates are controlled by (i) the concentration of sulphide or other oxidants in the water flowing in fractures contacting the buffer and (ii) diffusion across the buffer to the entire overpack surface area. The slow diffusion rates in saturated bentonite lead to such slow calculated corrosion rates that failure from corrosion should take orders of magnitude longer than the performance period. A conservative failure mode for corrosion focuses the available oxidant on a small area, which is only possible when focused advective transport dominates diffusion through the bentonite. Focused advective transport may occur when groundwater flow converges into a pipe through the bentonite. The assumption that a pipe has formed across the deposition hole within the bentonite, while contacting the copper surface en route, provides a conservative model to assess the consequences of fracture distributions, flow rates, and background sulphide concentrations. Such a pipe passes from an entry fracture and exits to the same or another fracture. A quantitative model illustrates the approach, taking into account the probability distribution of available background flow and hydraulic gradient in the fracture network to constrain the probability distribution of maximum pipe dimension and corresponding flow rates over all deposition holes. The model indicates that maximum local corrosion rates at early time may be many orders of magnitude larger than maximum local corrosion rates without a pipe, because the oxidant is delivered to an area many orders of magnitude smaller than the overpack area. Maximum local corrosion rates cannot be sustained, however, and drop rapidly as the corroding surface area expands over time.

I. INTRODUCTION

For geologic repositories in fractured saturated rocks (e.g., a granite host formation), a common design surrounds emplaced high-level radioactive waste canisters with a swelling bentonite buffer in order to (i) isolate the waste package from potentially corrosive formation waters, (ii) limit releases from failed waste packages, and (iii) support the waste packages during seismic and tectonic disturbances. The isolation function of diffusion-dominated transport in self-healing bentonite can be so dominant that performance is insensitive to the role of the barrier with respect to other factors.

The buffer isolation function limits canister corrosion rates so strongly that expected canister lifetimes may be orders of magnitude longer than the performance period. Other factors in the host environment may provide redundant performance benefits, but these cannot be easily quantified when canister performance is strongly dominated by diffusion within the buffer. Such factors are most easily quantified when the buffer has deteriorated in the most adverse fashion.

Within a deposition hole, diffusion-dominated transport of an oxidant from a fracture to the waste canister strongly dilutes the concentration of the oxidant relative to the background concentration. This dilution occurs because the cross-sectional area of the fracture is orders of magnitude smaller than the corroding canister surface area.

A consequence model that considers maximally adverse buffer performance delivers the oxidant at concentrations approaching the background concentration to a small fraction of the canister surface, because this locally increases corrosion rates. A hydraulic pipe through the buffer allows water to move through the buffer more rapidly, and may deliver substantially elevated oxidant concentrations to a small area of the canister wall if the pipe contacts the canister. Assuming that a hydraulic pipe is able to form in the buffer, its size, flow rate, and oxidant concentration should be consistent with environmental conditions in the host rock. Accordingly, a hydraulic pipe model may represent a maximally adverse buffer condition, allowing assessment of the barrier role of the host formation.

II. LIMITING MODELS FOR CORROSION OF A CANISTER IN A DEPOSITION HOLE

Several numerical models, developed using the COMSOL Multiphysics[1] numerical simulator, illustrate the roles of diffusion and advection in buffer performance. In all of the models, a single canister is assumed to be emplaced in a deposition hole. For purposes of illustration, the deposition hole and canister are assigned nominal properties proposed for the Swedish program[2]. The host rock is assumed to be sparsely fractured, with negligible matrix diffusion, so that only one fracture intersects the deposition hole. Two series of models are considered using the COMSOL simulator.

One series of models considers limiting behavior when the water in the deposition hole is essentially stagnant. For the purposes of illustration, the water at the fracture/deposition-hole interface is assumed to have the same oxidant concentration as the host rock far field. This assumption provides an upper-bound estimate for oxidant-limited corrosion rates. Ref. 2 considers similar scenarios, taking into account the change in concentration arising from diffusion within the host-rock fractures.

The second series of models considers limiting behavior when a defect in the buffer permits locally flowing water within the buffer. The water supply is constrained by the ability of the host rock to provide water. The defect is assumed to have evolved into the shape of a circular pipe, which is the most energetically favorable configuration when erosion shapes the defect. The pipe is assumed to contact the canister, providing the maximum consequence with respect to corrosion.

II.A. Diffusion-Limited Corrosion of a Canister in a Deposition Hole

Scenarios with several different buffer and fracture configurations illustrate the interplay between buffer characteristics and delivery of oxidant from a fracture in the host formation. Each scenario considers the same copper canister and deposition hole, but the nature of the buffer and fracture differs. In all scenarios, the oxidant is assumed to be at the background concentration in the fracture (negligible resistance to diffusion in the fracture) and have zero concentration everywhere on the canister surface (corresponding to maximum corrosion rate given the oxidant supply).

In most scenarios, oxidant uptake on the canister changes slowly with position on the canister, and canister penetration is essentially one-dimensional (1D). This condition is violated at a canister corner or if oxidant is delivered through a defect much thinner than the copper cladding, altering the progress of the corrosion front because of converging (at the corner) and diverging (at the defect) diffusion patterns. The effects of local diffusion control on canister penetration are approximately described with simple models.

II.A.1 Cylindrical Model

The model domain consists of the deposition hole outside the canister, treated as a two-dimensional (2D) axisymmetric domain. All water in the domain is assumed stagnant, thus the physical process considered is molecular diffusion from the fracture source (with a fixed concentration) to the copper surface (zero concentration). For the purposes of illustration, the diffusion coefficient of an intact buffer is assumed to be an order of magnitude smaller than diffusion in stagnant water. This assumption likely over-estimates the contrast between the two media.

Five representative variants are considered, using the configurations in Fig. 1:

- A 1-mm fracture at the canister midpoint with an intact buffer ($D = 10^{-10}$ m^2/s)
- A 1-mm fracture at the canister midpoint with no buffer ($D = 10^{-9}$ m^2/s)
- A 1-mm fracture at the canister bottom with an intact buffer ($D = 10^{-10}$ m^2/s)
- A spalled zone along the entire deposition hole with an intact buffer ($D = 10^{-10}$ m^2/s) and uniform concentration at the deposition hole wall
- A 1-mm fracture and 1-mm seam through the buffer at the canister midpoint ($D = 10^{-10}$ m^2/s for buffer, $D = 10^{-9}$ m^2/s in seam)

The first two scenarios represent a base case, with the fracture far from a corner. The third and fourth scenarios preferentially attack a canister corner. The fifth case preferentially attacks a small region of the canister shell.

If a protocol were in place to avoid placement in deposition holes with observed fractures, the 1-mm fracture may be larger than would be encountered, but smaller fractures are difficult to grid effectively because of large differences in scale. In all of the scenarios, the fracture system supplies sulphide (the oxidant) to the fracture opening (or the spalled zone) at a concentration of 10^{-5} mol/L. This assumption is questionable in the spalled scenario. A permeable spalled zone is likely to induce flow within the spalled zone, advecting oxidant into the spalled zone, but water flow is likely to diminish rapidly away from the fracture. Diffusion into the deposition hole will progressively deplete the available oxidant in the spalled zone with distance from the fracture, so the spalled scenario may substantially overestimate total sulphide influx to the deposition hole.

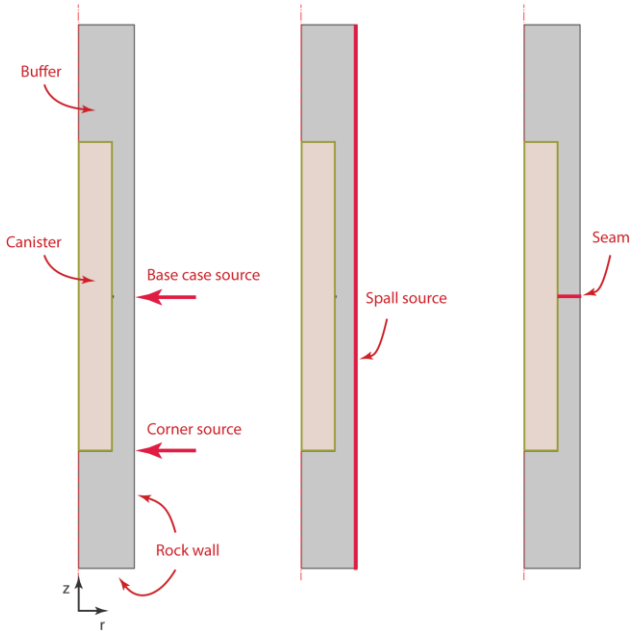

Fig. 1. Schematic description of 2D radial model geometry for the deposition hole and canister, including source location scenarios.

II.A.2 Local Diffusion Control at the Canister Surface

Sulphide from the background groundwater environment supplied to the copper canister surface balances copper dissolution at the rate of two moles of copper to one mole of supplied sulphide. Copper canister breakthrough occurs when 5 cm of copper is dissolved at some location on the canister surface, completely penetrating the copper shell. In the example scenarios, corroded copper readily diffuses away from the canister without restricting corrosion rates.

The base-case source scenarios (see Fig. 1) deliver oxidant to the canister with local fluxes varying little at scales comparable to the copper shell thickness, thus penetration estimates in these scenarios directly use molecular flux rates at the canister surface as calculated by COMSOL to calculate copper loss.

The corner source and spalled zone scenarios have a peak initial rate at the corner, and the corner is attacked from both the bottom and side (convergent diffusion to the corner). This dual attack tends to round the initially square corner, but the distance from the corner to the canister interior is 7.1 cm ($\sqrt{2}$ times the canister wall thickness). As an approximate estimate of penetration time, penetration is assumed to occur when a quarter torus with radius of 7.1 cm is removed with the initial molecular flux rates attacking the cylinder corner within this radius.

The seam defect scenario delivers elevated fluxes of the oxidant to the canister surface in a zone that is only 2 percent of the copper thickness. In this case, initial corrosion rates are rapid but narrow, forming a semicircular groove around the canister. However, the groove expands radially because the oxidant diffusing from the seam to the expanding surface preferentially attacks the nearest surface. As an approximate estimate, penetration occurs when the volume of half a torus with radius of 5 cm is removed, using the molecular flux rates initially attacking the canister within a 5-cm distance from the seam.

II.A.3 Representative Results

Fig. 2 illustrates the instantaneous corrosion rate of the canister surface and the time to penetration using the instantaneous rate. The ratio of the peak rate to surface-average rate is indicated in the legend to Fig. 2. For comparison purposes, the position axis is centered on the location of the peak instantaneous rate. The time of penetration adjusted for converging and diverging diffusion is indicated with circles in the bottom figure. These calculated estimates are proportional to the background concentration, thus increasing the background concentration would proportionately decrease the breakthrough time.

All of the considered cases have an initial breakthrough time between 25 and 250 million years, without considering constraints in the fracture system. The corner scenario is a reasonable bounding geometry, but the position of the fracture only modestly affects the penetration time (penetration is less than 3 times more rapid with the corner scenario than the midpoint scenario with the same buffer). A diffusion coefficient of pure water (rather than buffer) is arguably the bounding case under diffusion-controlled conditions. Even so, complete absence of a buffer is likely to increase the corrosion rate by less than the modeled factor of 10, because (i) the actual diffusion coefficient contrast is probably smaller and (ii) the fracture system would tend to constrain delivery of the oxidant to a greater extent.

Note that the spalled zone scenario likely supplies more oxidant than would be physically realistic if the same fracture were considered for all of the scenarios. If diffusion in the spalled zone were explicitly represented, the corrosion profiles would probably be a smeared version of the base-case or corner scenarios.

The seam defect scenario illustrates that delivery of the oxidant to a small area can greatly increase the initial

corrosion rate, but constraints on the shape of the corroding front imposed by diverging diffusion greatly slow the progress of the front over time and the penetration time is only modestly more rapid than would occur with an intact buffer.

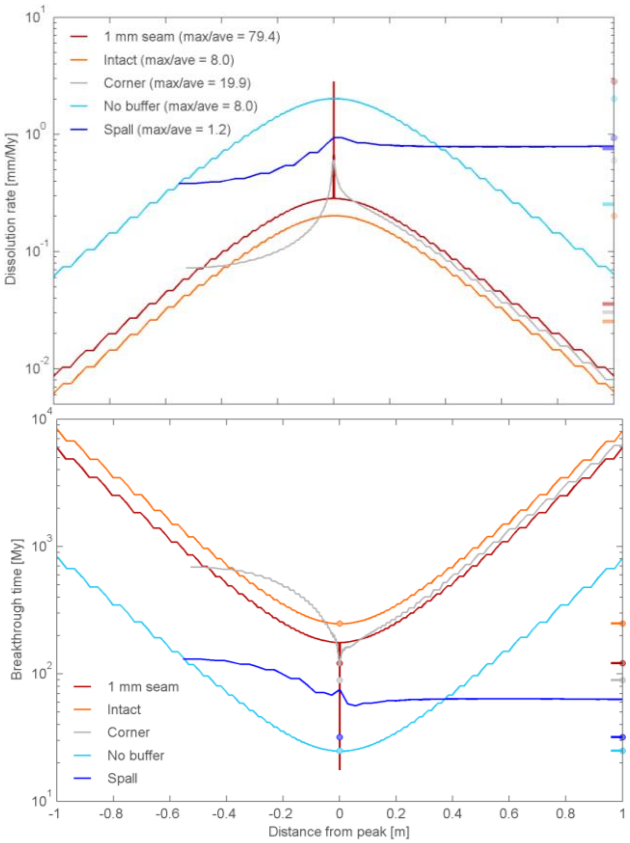

Fig. 2. Spatial distribution, relative to the peak location, of (top) instantaneous corrosion rate and (bottom) corresponding time to penetrate a 5-cm copper thickness given a 10^{-5} mol/L sulphide background concentration. Symbols on right axis of (top) indicate peaks (circles) and averages across the entire canister surface (bars). Circles in (bottom) indicate average corrosion rate, correcting for radial diffusion at corners and seam endpoint.

II.B. ADVECTION-CONSTRAINED CORROSION OF A CANISTER WITH A HYDRAULIC PIPE

In laboratory experiments, pipes have been observed forming along cylinder walls during bentonite rewetting experiments with constant applied flow rates[3]. In the experiments, bentonite removal rates drop rapidly with time as the pipe develops but colloidal removal arguably continues at low rates for long periods. Observed pipes are associated with soft gel during the swelling process[4]. Although the imposed conditions in the laboratory experiments may be more extreme than would be expected under field conditions, the fact that pipes were observed forming in a bentonite experiment suggests a conceptual model for advection-dominated corrosion that operates in the small contact areas where a hydraulic pipe contacts the canister.

Under the hydraulic conditions expected near a deposition hole in sparsely fractured granite, hydraulic pipes might have a diameter on the order of millimeters, thus representing very small physical defects in the buffer with little bentonite mass removed into the fracture system to potentially block the flow system. The pipe diameter depends on the flow rate and hydraulic gradient, which in turn depend on the background hydraulic gradient and the fracture aperture feeding the pipe. Accordingly, the pipe model provides a consequence model that directly depends on the host formation.

This scenario provides an extreme consequence model, because a hydraulic pipe would tend to deliver the oxidant to a small area of the canister surface. However, the oxidant also diffuses from the pipe into the buffer, so the oxidant may deplete before slow flows reach the canister. Accordingly, the pipe model also depends on the buffer characteristics. As with the seam scenario, a hydraulic pipe would deliver oxidant to a small area of the canister. Local diffusion control near the canister surface would also apply for a pipe model.

II.B.1 Pipe Model

The hydraulic pipe diameter is orders of magnitude smaller than the canister and deposition hole diameters. Gridding is extremely challenging in three dimensions with the wide range in scales. Accordingly, the model domain is an abstracted representation of the hydraulic pipe, deposition hole, and canister.

The simplified system shown in Fig. 3 considers (i) a straight cylindrical pipe with constant radius, (ii) a surrounding bentonite cylinder, and (iii) the outer edge of the canister essentially tangent to the pipe. The canister carves out part of the bentonite cylinder. The pipe and bentonite cylinders have the same length as the deposition-hole diameter. If the deposition-hole geometry was considered, a curved section would be missing on both ends of the bentonite cylinder.

The analytic velocity distribution within the cylindrical pipe is parabolic, assuming that flow is laminar and constant. The sulphide concentration is fixed at the background value at the inlet to the pipe, essentially assuming that diffusion within the fracture is overwhelmed by flow convergence. The copper canister and the outer edge of the bentonite cylinder are assumed

to have zero concentration, maximizing diffusion from the pipe.

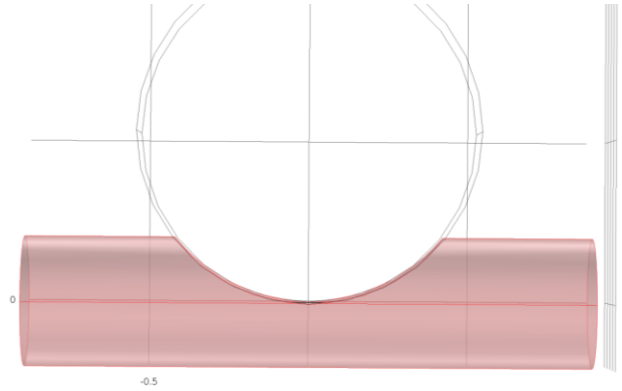

Fig. 3. Geometry of the pipe simulation. The highlighted zone is the simulation domain, representing a bentonite cylinder cut by a canister. The pipe is located at the bentonite cylinder centerline. Deposition-hole boundaries are neglected at the ends of the simulation domain.

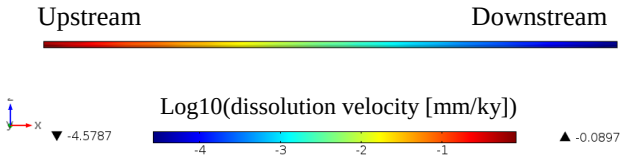

Fig. 4. Rate of copper removal along the 9.2-cm strip of a 1-mm diameter pipe where it grazes the canister. The color scale indicates instantaneous dissolution velocity; extremes values are indicated with triangles. Flow is from left to right.

To represent the scenario of a pipe glancing along the canister wall, which over time would cut a semi-circular groove into the copper, the pipe centerline passes 2 mm inside the outer boundary of the copper shell. To overcome gridding constraints, a cylindrical region with ten times the radius of the pipe surrounds the pipe, forming a groove in the copper shell where it overlaps. Half of the pipe exterior facing the copper shell has a zero-concentration boundary to represent copper contact.

Fig. 4 illustrates the distribution of initial dissolution rate along the portion of the hydraulic pipe contacting the copper surface. The pipe has a nominal 1 mm diameter, with an average pipe velocity of 2000 m/yr and background sulphide concentration of 10^{-5} mol/L. The dissolution rate represents general corrosion, not pitting corrosion, even though the peak dissolution rate is highly localized. The local removal rate decreases exponentially from 0.81 to $2.6 \cdot 10^{-5}$ mm/ky over the 9.2-cm length of the exposed zone, and the peak dissolution rates occur in only a few square millimeters. If it were physically possible to maintain the peak dissolution rate on the same small area, the canister would breach in approximately 61,000 years.

II.B.2 Local Diffusion Control at the Canister Surface

Assuming that (i) the actual penetration excavates a spherical depression in the copper surface and (ii) the initial volumetric rate of copper removal Q (i.e., volume/time) as estimated by transfer from the pipe to the exposed copper remains constant, a shell balance can be integrated to estimate the time required for a hemisphere to increase to 5 cm radius. Half the surface area of a sphere with 5-cm radius is $1.57 \cdot 10^4$ mm^2, thus the final dissolution rate is roughly 4 orders of magnitude slower than initial peak dissolution rate.

The rate of expansion of a spherical shell with a constant molecular flux $2Q$ is

$$\frac{dr}{dt} = \frac{2Q}{A} = \frac{2Q}{4\pi r^2} \qquad (1)$$

where r is the radius, t is time, and A is the area of the shell. Rearranging and integrating,

$$T = \int_0^T dt = \int_0^R \frac{2\pi r^2}{Q} dr = \frac{2\pi R^3}{3Q} \qquad (2)$$

In this relationship, R is the thickness of the copper shell and T is time for first penetration. This provides a geometric scaling to calculate penetration time from the initial delivery rate of sulphide from the pipe to the entire exposed copper surface.

Fig. 5 illustrates sensitivity results for combinations of pipe diameter and velocity. The results are expressed as time for dissolution to penetrate 5 cm at (i) the initial peak dissolution rate and (ii) accounting for diffusion-limited growth of a hemispherical shell. The horizontal axis in Fig. 5 is the incoming concentration times the volumetric flow rate in the pipe. In Fig. 5, symbols labelled with c_0 represent simulation results using a background concentration of 10^{-5} mol/L and symbols labelled with $c_0/5$ or $c_0 \times 5$ are calculated by simply scaling the input flux and failure time.

The initial peak dissolution rate estimate is somewhat affected by gridding, but roughly scales with the inverse of the pipe diameter. This is consistent with the same total consumption spread over an area proportional to the pipe diameter. The different pipe diameters result in similar total sulphide delivery to the copper surface, based on the similar time to penetration when the spherical integration is considered.

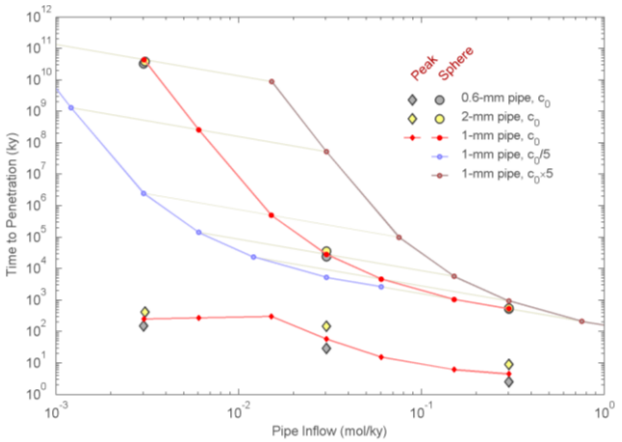

Fig. 5. Time to penetrate 5 cm of copper given pipe supply of sulphide at (i) the initial peak dissolution rate and (ii) with diffusion-limited growth of a hemispherical shell.

There is a clear transition from advection domination to diffusion domination as the pipe flux decreases. Diffusion domination occurs when pipe flux is below 0.015 mol/yr, left of the distinct break in the slope of peak initial dissolution rate. Advection domination occurs when pipe flux is above roughly 0.15 L/yr, marked by a flattening in the slope of peak initial dissolution rate. The sphere penetration time scales with flux as

$$\frac{T_2}{T_1} = \left(\frac{Q_1}{Q_2}\right)^{\alpha} \qquad (3)$$

where Q is oxidant inflow rate to the pipe and T is time to penetration. In the simulation results, the exponent α increases from 1 in the advection dominated regime to more than 7 in the diffusion dominated regime.

III. PROBABILISTIC CONSEQUENCE MODEL

The hydraulic pipe model provides a means for assessing the degree to which the host rock provides a barrier capability to corrosion. For this purpose, it is reasonable to assume that a maximally adverse buffer defect occurs when (i) each deposition hole contacted by a flowing fracture has a single hydraulic pipe that grazes the canister, with the pipe diameter and pipe flow consistent with the flow field in the adjacent host rock, and (ii) erosion of the swelling bentonite gel somehow maintains the open defect over long periods of time.

III.A. Hydraulic Pipe Size and Host Formation Flow

Without speculating on how a pipe would initially form through a bentonite buffer, it is possible to estimate pipe characteristics consistent with site hydrological conditions.

Under laminar conditions, the average velocity of water in a pipe, v_{ave}, is

$$v_{ave} = \frac{\rho g r^2}{8\mu}\frac{dh}{dx} \qquad (4)$$

where ρ is density, g is the acceleration due to gravity, r is the pipe radius, μ is viscosity, and dh/dx is the head gradient in the pipe. Total volumetric flux in the pipe is

$$Q = \pi r^2 v_{ave} \qquad (5)$$

$$Q = \frac{\pi\rho g}{8\mu} r^4 \frac{dh}{dx} \qquad (6)$$

It is clear that the pipe radius strongly influences both the flux through the pipe and the velocity within the pipe.

The flow through a pipe is constrained by the hydraulic conditions in the surrounding fracture system. Assuming that a single pipe intercepts flow, an approximate upper bound on pipe flow might be the amount of flow intercepted by half the diameter of the deposition hole, with the remainder diverting laterally around the deposition hole. Similarly, the surrounding fracture system constrains the hydraulic gradient in the pipe not to be much larger than the background hydraulic gradient. A smaller hydraulic gradient would imply that some funneling into the pipe is occurring, with the degree of funneling constrained by the velocity required for the erosion necessary to maintain an open pipe in the face of bentonite swelling.

Assuming that the worst-case scenario is the upper bound pipe flux, the minimum pipe radius is

$$r_{min} = \left[\frac{Q_{max}}{(dh/dx)_{bg}}\frac{8\mu}{\pi\rho g}\right]^{1/4} \qquad (7)$$

The maximum average velocity through the pipe occurs with the minimum radius, leading to

$$v_{max} = \frac{Q_{max}}{\pi r_{min}^2} \qquad (8)$$

It may be adequate to use flow from approximately the separation distance between deposition holes to estimate maximum flux to estimate consequences.

III.B. Representative Results

The hydraulic pipe approach is useful for assessing the barrier capability offered by the host rock, and is readily applied to discrete fracture model estimates. To illustrate the approach, the hydraulic pipe method is

applied to one realization of a probabilistic discrete fracture model created by the Swedish Nuclear Fuel and Waste Management Company (SKB). SKB uses CONNECTFLOW to perform discrete fracture modeling. Circular planar fractures down to 0.4 m radius are included in the model close to the repository, and large fractures are tessellated to 10 m length[5]. An SKB base realization describes the main fracture intersecting the deposition hole at 6916 modeled deposition holes[6]. Most (60 percent) of the holes had no intersecting fracture or zero modeled flow. Fig. 6 (top) indicates the modeled fracture-average volumetric fluxes and apertures and Fig. 6 (bottom) indicates estimated hydraulic gradients. Hydraulic gradients are estimated assuming transmissivity is proportional to the fracture aperture squared. Each deposition hole has the same symbol in Figs. 6 through 8 to aid comparison. Note that the largest fractures in this realization would be quite visible and could disqualify the deposition hole as a candidate for canister emplacement.

Fig. 7 shows that the distribution of calculated r_{min} and v_{max} values are poorly correlated with the fracture fluxes and gradients shown in Fig. 6, using the same color coding. Two lines are drawn for each deposition hole to indicate bounds on how velocity might respond as the pipe radius increases, and thereby decreases the hydraulic gradient within the pipe that is necessary to carry a given flux. Both lines consider the consequences of reducing the gradient in the pipe by an order of magnitude relative to the background gradient. The slanted lines neglect additional funneling to the pipe, while the horizontal lines assume that reducing the pipe gradient corresponds to a proportional increase in the background flow that is funneled to the pipe. Given that the spacing between deposition holes is approximately 7 times the deposition-hole radius, an order of magnitude increase in flux funneled to the pipe may be a reasonable upper bound.

The example is based on a 1-mm diameter pipe carrying flow of 1.6 L/yr at a background concentration of 10^{-5} mol/L. Assuming that all flow is captured in a width equal to the canister radius, this flow rate is exceeded at approximately 1 percent of the deposition holes. To examine sensitivity, three velocity scenarios (multiplying the base rate by 0.1, 1, and 10) and three pipe diameters (0.6, 1, and 2 mm) are considered (shown in Fig. 5). These nine cases are labeled "Simulation case" in Fig. 7, with the nominal case in the middle. The nominal case is also considered with background concentrations that are multiples of the nominal background concentration.

Fig. 8 (top) illustrates the penetration time for a corrosion hemisphere for the set of pipes, using the same color coding as Fig. 6. The sulphide concentration entering the pipe is 10^{-5} mol/L; penetration time is inversely proportional to background concentration. The penetration time calculation assumes that all background sulphide is funneled into the pipe (diffusion to the buffer within the fracture system is negligible). This assumption overestimates pipe delivery rates. A substantial amount may diffuse directly from the fracture to the buffer at low flow rates, similar to the intact-buffer scenario.

Fig. 8 (bottom) compares the time of penetration with pipe flow to the time of penetration for diffusion through an intact buffer for the same deposition hole (i.e., using the simulation results shown in Fig. 2). The crossover between advection and buffer diffusion as the dominant behavior occurs when the pipe has a flow rate of approximately 1 L/yr. As diffusion in the fracture system (not the buffer) tends to be limiting at low flows, the crossover point may occur at even smaller flow rates.

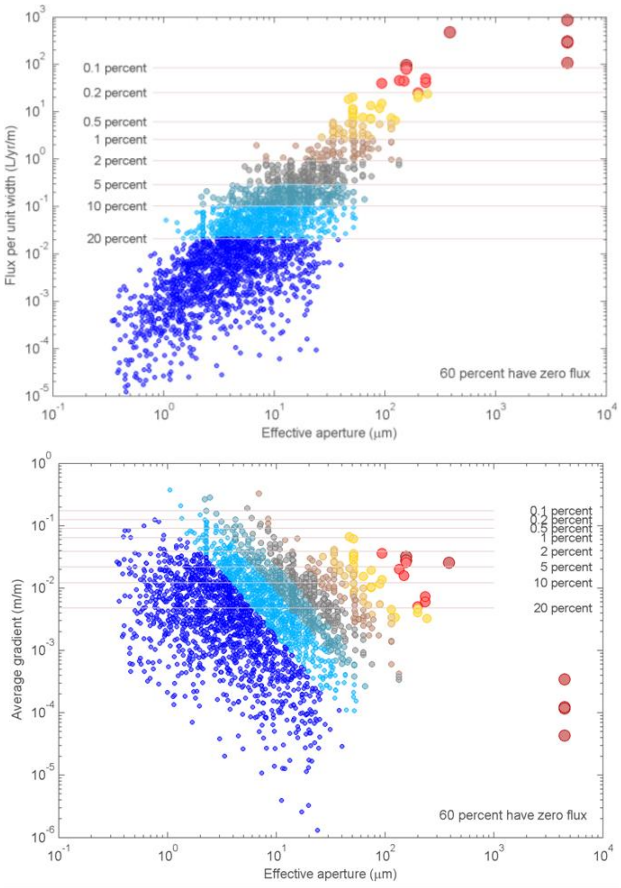

Fig. 6. Simulation results for (top) flux per unit width and (bottom) average gradient. Colors denote flux frequency.

Fig. 8 suggests that pipe flow (if it occurred) would yield shorter penetration times than the nominal scenario for 5 to 10 percent of the deposition holes. However, only approximately 0.5 percent of the deposition holes would experience a penetration time shorter than one million years, and such holes are likely candidates for screening by visual inspection.

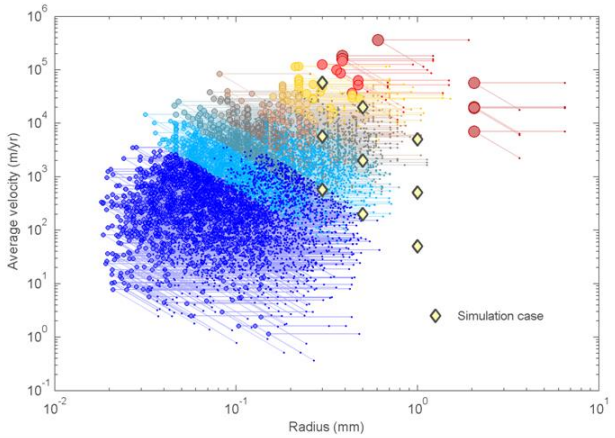

Fig. 7. Scatter plot of limiting pipe radius and velocity given fracture fluxes and gradients at deposition holes. Symbols use the color scheme from Fig. 6. Lines illustrate the consequence of reducing pipe gradient one order of magnitude relative to background with flux capture multiplied by 1 (slant) and 10 (horizontal).

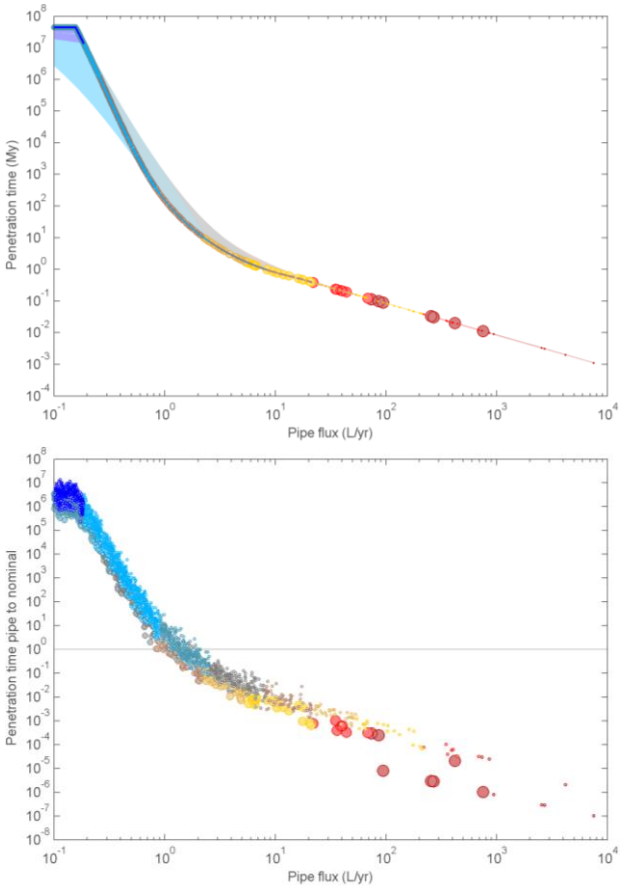

Fig. 8. (top) Estimated penetration time as a function of volumetric flux in the pipe for spherical dissolution at the pipe/copper contact. (bottom) Ratio of penetration times for pipe flow relative to the nominal intact buffer scenario with a 1-mm fracture (see Fig. 2).

IV. CONCLUSIONS

Two types of bounding models were developed for canister corrosion in a deposition hole within a fractured host rock. The first set of bounding models considered corrosion limited by diffusion in the deposition hole, which provides protection for extremely long durations. These scenarios reveal that ensuring diffusion dominance is a key function of the buffer. This function may also be achieved without any buffer in large deposition holes when large fractures are precluded.

Diffusion dominance in the deposition hole masks the host-formation barrier capability. The second model probes this barrier capability by considering a hypothetical hydraulic pipe through the buffer, controlled by flow in the host rock. The hydraulic pipe model estimated a decrease in penetration time by up to several orders of magnitude in the few deposition holes with large hydraulic pipes. For most holes, the equilibrium hydraulic pipe delivers oxidant at such a small rate that a nominal intact buffer scenario (with a 1-mm fracture) estimates faster penetration times.

ACKNOWLEDGMENTS

The work presented here was funded in part by the Swedish Radiation Safety Authority (SSM). This paper is an independent product of the CNWRA and does not necessarily reflect the regulatory position of SSM.

REFERENCES

1. COMSOL Multiphysics Version 4.3a, COMSOL.
2. I. NERETNIEKS, L. LIU, and L. MORENO. *Mass transfer between waste canister and water seeping in rock fractures. Revisiting the Q-equivalent model.* SKB TR-10-42, Svensk Kärnbränslehantering AB (2010).
3. T. SANDÉN and L. BÖRGESSON. *Early effects of water inflow into a deposition hole.* SKB R-10-70, Svensk Kärnbränslehantering AB (2010).
4. SKB. *Buffer, backfill and closure process report for the safety assessment SR-Site.* SKB TR-10-47, Svensk Kärnbränslehantering AB (2010).
5. S. JOYCE, T. SIMPSON, L. HARTLEY, D. APPLEGATE, J. HOEK, P. JACKSON, D. SWAN, N. MARSIC, and S. FOLLIN. *Groundwater flow modelling of periods with temperate climate conditions – Forsmark.* SKB R-09-20, Svensk Kärnbränslehantering AB (2010).
6. SSM2011-2426-130. Excel file "hydrogeological_base_case_r0_velocity.xls". SKBdoc id 1396328 ver 1.0, Svensk Kärnbränslehantering AB (2011).